Article

Cell

Dual Chromatin and Cytoskeletal Remodeling by SETD2

Graphical Abstract

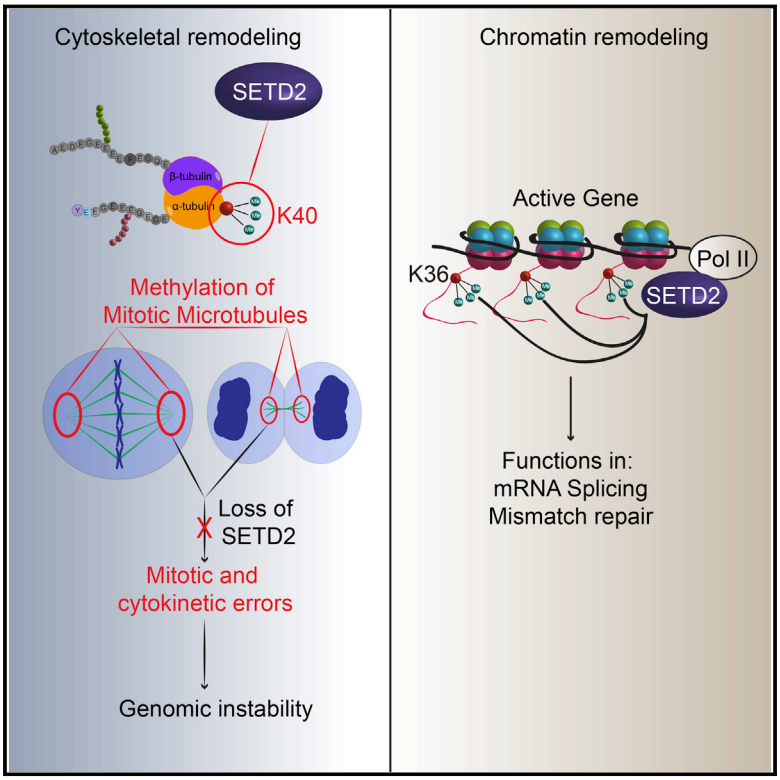

Highlights

- Dynamic microtubules are methylated during mitosis and cytokinesis
- SETD2 methylates α-tubulin at lysine 40, the same lysine that is acetylated
- Loss of microtubule methylation causes genomic instability

Authors

In Young Park, Reid T. Powell, Durga Nand Tripathi, ..., Eric Jonasch, W. Kimryn Rathmell, Cheryl Lyn Walker

Correspondence

cherylw@bcm.edu

In Brief

Tubulin and histones share a methyltransferase, suggesting a new basis for known tumorigenic mutations in the enzyme.

Park et al., 2016, Cell *166*, 950–962
August 11, 2016
http://dx.doi.org/10.1016/j.cell.2016.07.005

CellPress

Cell

Article

Dual Chromatin and Cytoskeletal Remodeling by SETD2

In Young Park,[1,9,10] Reid T. Powell,[1,9,10] Durga Nand Tripathi,[1,10] Ruhee Dere,[1,10] Thai H. Ho,[2] T. Lynne Blasius,[3] Yun-Chen Chiang,[4] Ian J. Davis,[4,5] Catherine C. Fahey,[4] Kathryn E. Hacker,[4] Kristen J. Verhey,[3] Mark T. Bedford,[6] Eric Jonasch,[7] W. Kimryn Rathmell,[4,8] and Cheryl Lyn Walker[1,10,*]

[1]Center for Translational Cancer Research, Institute of Biosciences and Technology, Texas A&M Health Science Center, Houston, TX 77030, USA

[2]Division of Hematology/Oncology, Mayo Clinic Arizona, Scottsdale, AZ 85259, USA

[3]Department of Cell and Developmental Biology, Medical School, University of Michigan, Ann Arbor, MI 48109, USA

[4]Department of Genetics and Lineberger Comprehensive Cancer Center, University of North Carolina, Chapel Hill, NC 27599, USA

[5]Department of Pediatrics, University of North Carolina, Chapel Hill, NC 27599, USA

[6]Department of Epigenetics and Molecular Carcinogenesis, The University of Texas MD Anderson Cancer Center, Smithville, TX 78957, USA

[7]Department of Genitourinary Medical Oncology, The University of Texas MD Anderson Cancer Center, Houston, TX 77030, USA

[8]Division of Hematology/Oncology, Vanderbilt-Ingram Cancer Center, Vanderbilt University, Nashville, TN 37232, USA

[9]Co-first author

[10]Present address: Department of Molecular and Cell Biology, Baylor College of Medicine, Houston, TX 77030, USA

*Correspondence: cherylw@bcm.edu

http://dx.doi.org/10.1016/j.cell.2016.07.005

SUMMARY

Posttranslational modifications (PTMs) of tubulin specify microtubules for specialized cellular functions and comprise what is termed a "tubulin code." PTMs of histones comprise an analogous "histone code," although the "readers, writers, and erasers" of the cytoskeleton and epigenome have heretofore been distinct. We show that methylation is a PTM of dynamic microtubules and that the histone methyltransferase SET-domain-containing 2 (SETD2), which is responsible for H3 lysine 36 trimethylation (H3K36me3) of histones, also methylates α-tubulin at lysine 40, the same lysine that is marked by acetylation on microtubules. Methylation of microtubules occurs during mitosis and cytokinesis and can be ablated by *SETD2* deletion, which causes mitotic spindle and cytokinesis defects, micronuclei, and polyploidy. These data now identify SETD2 as a dual-function methyltransferase for both chromatin and the cytoskeleton and show a requirement for methylation in maintenance of genomic stability and the integrity of both the tubulin and histone codes.

INTRODUCTION

SET-domain-containing 2 (SETD2), also known as HYPB and KMT3A, is a histone methyltransferase responsible for histone H3 lysine 36 trimethylation (H3K36me3) of chromatin, an epigenetic mark associated with gene transcription (Edmunds et al., 2008; Hu et al., 2010). It is also one of the many "readers, writers, and erasers" of the histone code (Jenuwein and Allis, 2001; Strahl and Allis, 2000), which is comprised of post-translational modifications (PTMs) including acetylation, phosphorylation, ubiquitination, and methylation of multiple sites on histone tails, which together constitute a complex language for transcriptional regulation (Lee et al., 2010). SETD2 is able to add a methyl group to a di-methylated lysine to generate a trimethyl mark, as well as de novo mono- and di-methylation to generate a trimethyl mark on histone H3 (Wagner and Carpenter, 2012; Yuan et al., 2009). H3K36me3 of chromatin is a non-redundant SETD2 function (Edmunds et al., 2008), and loss of SETD2 is embryonic lethal (Hu et al., 2010).

Recently, the concept of the "histone code" has been parlayed into a "tubulin code" hypothesis to describe how PTMs distinctly mark subsets of microtubules in the cytoskeleton (Verhey and Gaertig, 2007). The cytoskeleton is a network of fibers that maintains cell shape, allows cells to move and divide, and forms specialized structures such as cilia and microvilli. Although the name implies a stable structure, many parts of the cytoskeleton are dynamic and constantly remodeled, with some parts assembled while others are dismantled. An important component of the cytoskeleton is microtubules, which are built from heterodimers of α- and β-tubulin and are required for many diverse functions such as mitosis, where they form the mitotic spindle and participate in chromosome segregation and cytokinesis (Walczak and Heald, 2008). The "tubulin code" hypothesis posits that PTMs of specific tubulin subunits within the polymer direct microtubule-based functions at that location (Verhey and Gaertig, 2007). Indeed, PTMs including phosphorylation, detyrosination, polyglutamylation, polyglycylation, and acetylation are enriched on specialized microtubule structures such as centrioles and basal bodies, neuronal axons, and primary cilia (Janke, 2014; Song and Brady, 2015).

Most microtubule PTMs have been discovered serendipitously, usually as the result of generation of antibodies later found to react with specific modified residues of α- or β-tubulin (Magiera and Janke, 2013), and as a result, the complete repertoire of microtubule PTMs has yet to be fully elucidated. PTMs of

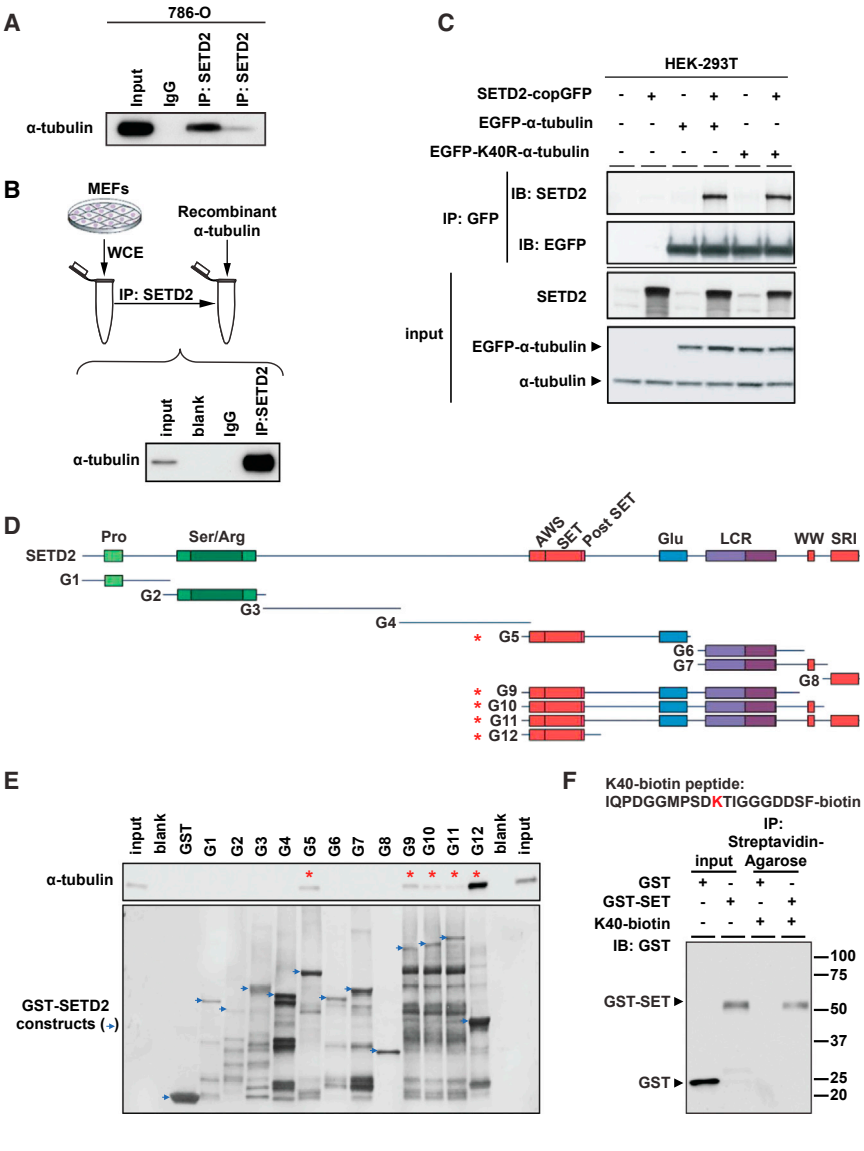

Figure 1. SETD2 Binds α-Tubulin

(A) Co-immunoprecipitation of endogenous α-tubulin and SETD2 from 786-0 cells with two different SETD2 antibodies (Sigma-Aldrich and Abcam).

(B) Co-immunoprecipitation of immunopurified SETD2 from MEFs using SETD2 antibody and recombinant α-tubulin. Input, recombinant α-tubulin, 10 ng.

(C) Co-immunoprecipitation of exogenous SETD2 and α-tubulin from HEK293T cells co-expressing SETD2 and EGFP-α-tubulin or EGFP-K40R-α-tubulin.

(D) Schematic of GST-SETD2 fusion protein constructs.

(E) GST pull-down assays of α-tubulin with the GST-SETD2 fusion constructs incubated with 1 μg recombinant α-tubulin (TUBA1A) protein and immunoblotted using α-tubulin antibody (top). GST-SETD2 construct expression was assessed using Coomassie blue staining (bottom).

(F) Peptide pull-down using biotin-labeled K40 peptide of α-tubulin with the G12 or GST-only constructs. Input, 50 ng.

microtubules serve many functions, such as recognition by microtubule-associated proteins (MAPs), which can regulate microtubule dynamics and function. These modifications play important roles during mitosis, where, for example, detyrosination guides chromosome congression (Barisic et al., 2015). However, for many PTMs, the underlying functionality is still undetermined (Janke, 2014; Song and Brady, 2015). Compared to PTMs that specify stable cytoplasmic microtubules, which are easily detected by purification or immunoreactivity with PTM-specific antibodies, little is known about PTMs associated with mitotic spindle and midbody microtubules that direct their dynamic polymerization and depolymerization during mitosis (Kwok and Kapoor, 2007; Walczak and Heald, 2008).

Importantly, the readers, writers, and erasers of the histone and tubulin codes identified to date have been distinct, even for PTMs such as acetylation that occur on both histones and microtubules. As a result, in settings such as cancer, where defects in chromatin remodelers such as *SETD2* occur with a high frequency, research to understand how loss of readers, writers, and erasers such as SETD2 contribute to disease pathogenesis has focused on chromatin and the impact of loss of H3K36me3 on the epigenome.

We have now found that SETD2 is required for the integrity of both the histone and tubulin codes, providing evidence for cross-talk between the epigenome and cytoskeleton. We show that methylation is a PTM of mitotic microtubules and that SETD2 binds to and methylates α-tubulin. Methylation occurs at lysine 40 (α-TubK40me3), the same residue that is acetylated on microtubules (α-TubK40ac). Methylation occurs on the spindle during mitosis and the midbody during cytokinesis, and *SETD2*-null cells exhibit loss of spindle and midbody methylation and numerous mitotic and cytokinesis defects, identifying a role for microtubule methylation by SETD2 in genomic stability.

RESULTS

SETD2 Binds α-Tubulin

We found that endogenous SETD2 could be co-immunoprecipitated with α-tubulin in *SETD2*-proficient human 786-0 cells (Figure 1A). A direct interaction between SETD2 and α-tubulin was demonstrated by incubating SETD2 protein immunopurified using a SETD2-specific antibody with human recombinant α-tubulin protein (TUBA1A), followed by co-immunoprecipitation (coIP) of α-tubulin (Figure 1B).

SETD2 binding and H3K36 methylation of histone tails coincides with histone acetylation at active genes (Edmunds et al.,

2008), leading us to ask if acetylation, which is known to occur on microtubules, might play a role in SETD2 binding to α-tubulin. Treatment of cells with trichostatin A (TSA), a histone deacetylase (HDAC) inhibitor that selectively inhibits class I and II mammalian HDACs, including the α-tubulin deacetylase HDAC6 (Matsuyama et al., 2002), had no effect on SETD2 binding to α-tubulin (data not shown), and co-expression of wild-type EGFP-α-tubulin and mutant EGFP-K40R α-tubulin (which cannot be acetylated) with full-length SETD2 revealed that SETD2 could co-immunoprecipitate with both wild-type and K40R mutant α-tubulins, indicating that the interaction of SETD2 with α-tubulin did not require acetylation of K40 (Figure 1C).

To determine the α-tubulin binding domain of SETD2, we constructed a series of glutathione S-transferase (GST) fusion proteins containing human SETD2 fragments purified from *Escherichia coli* (Figures 1D and 1E). While SETD2 protein levels expressed from various constructs differed, we consistently observed that the presence of the SET (*Drosophila* Su(var)3–9 and "Enhancer of zeste" proteins) domain was required for binding to α-tubulin. As shown in Figure 1E, GST pull-down assays revealed that the SET domain was sufficient for binding to α-tubulin, consistent with an enzyme-substrate relationship.

To identify potential sites for methylation on lysine residue(s) of tubulin, we analyzed the amino acid sequence of α-tubulin for motifs that fit the structural requirements for substrates of SETD2 and its corresponding demethylase, JMJD2A (also known as KDM4A, JHDM3A, and TDRD14A). The catalytic domain of both SETD2 and JMJD2A requires a curved or flexible structure containing Pro at +2 or Gly-Gly at +3 and +4 after the substrate lysine residue (Chen et al., 2007; Nelson et al., 2006). We found only one candidate lysine within α-tubulin that met these structural requirements, K40, where the sequence "**K**TI**GG**" is a good fit as a structural motif for a SETD2 or JMJD2A substrate. A biotin-tagged peptide around this region, IQPDGGMPSDKTIGGGDDSF-biotin, could co-immunoprecipitate a GST-tagged SET domain (Figure 1F). An antibody raised against the H3K36me3 epitope also could immunoprecipitate α-tubulin (Figure S1A), supporting this as a potential recognition site for SETD2 methylation.

To further confirm these data, we generated a polyclonal antibody against trimethylated K40 peptide of α-tubulin (α-TubK40me3). This antibody had minimal cross-reactivity with a di-methylated K40 peptide and no detectable cross reactivity with mono- or un-methylated K40 peptides (Figure S1B). We found that similar to the commercially available H3K36me3 antibody, the α-TubK40me3-specific antibody generated to the K40 peptide also detected and immunoprecipitated native α-tubulin (Figure S1A), indicating similarity between the trimethyl SETD2-epitope of chromatin and the methyl-specific epitope recognized by the α-TubK40me3-specific antibody. The specificity of the α-TubK40me3 antibody was demonstrated using a peptide competition assay where an α-TubK40me3 peptide strongly, and α-TubK40me2 peptide modestly, competed for binding of the α-TubK40me3-specific antibody to α-tubulin, with little loss of immunoreactivity seen with mono-methylated, acetylated, or unmethylated α-TubK40 peptides (Figure S1C).

Microtubule Methylation Occurs during Mitosis

Because binding of the SET domain to α-tubulin and recognition by both H3K36me3 and α-TubK40me3-specific antibodies suggested that SETD2 could be methylating microtubules, we immunostained mouse embryonic fibroblasts (MEFs) using either the α-TubK40me3-specific or H3K36me3 antibodies together with either α-tubulin (Figures 2A and 2B) or acetylated α-tubulin (Figures S2A and S2B). In mitotic cells, in addition to the expected immunostaining of chromatin, we observed distinct immunoreactivity with both the α-TubK40me3 and H3K36me3 antibodies on spindle microtubules, but not astral microtubules (Figures 2A, 2B, S2A, and S2B). During metaphase, methylation of spindle microtubules was concentrated near the spindle poles as shown in Figures 2A, 2B, S2A, and S2B and illustrated with a line profile through a representative metaphase spindle stained with α-TubK40me3 and α-tubulin antibodies (Figure S2C). Methylation at the minus ends of bundled microtubules becomes especially evident when the spindle midzone compacts into the midbody during cytokinesis (Figures 2A–2C, S2A, and S2B).

To further investigate the methylation state of spindle microtubules, we stained cells with a series of pan mono-, di-, and trimethyl lysine antibodies (Guo et al., 2014). In addition to the expected mono-, di-, and tri-methylation of chromatin (Figures 2, S2, and S3), we also observed immunoreactivity of spindle and midbody microtubules using a pan tri-methyl lysine (Kme3) antibody (Figure S3A), but not, however, with the pan mono-methyl (Kme1) or di-methyl (Kme2) lysine antibodies (Figures S3B and S3C). Antibodies to methyl lysine marks made by the other histone methyltransferases H3K4me3 (COMPASS complex) or H3K27me3 (EZH2) showed no immunoreactivity for these microtubule structures (Figure S3D). Together, these data identify a methylated epitope on mitotic microtubules recognized by the α-TubK40me3, H3K36me3, and pan-Kme3 antibodies rather than non-specific association of histones/chromatin with this structure.

A striking feature of microtubule trimethylation was the apparently exclusive relationship between trimethylation and the well-known α-tubulin K40ac mark, particularly during the later stages of mitosis. Co-staining with α-TubK40me3 and H3K36me3 and α-tubulin antibodies showed trimethylation on the distal, minus ends of midbodies distinct from chromatin H3K36me3 staining (Figures 2A–2C), while co-staining with α-TubK40me3, H3K36me3, and acetylated α-tubulin showed the methyl mark occurred more distally on the midbody than the acetyl mark (Figures S2A and S2B). As shown in Figure 2C, quantification (n = 66) of the fluorescence intensity of trimethyl- and acetyl-specific antibody staining along the length of the midbody revealed an inverse relationship between acetylation and trimethylation. This suggested the possibility that microtubule acetylation and methylation were reciprocal marks, and focused our attention on the site for microtubule acetylation, lysine 40 of α-tubulin (Janke, 2014; Verhey and Gaertig, 2007).

SETD2 Methylates Lysine 40 of α-Tubulin

To examine whether methylation at K40 of α-tubulin occurs in vivo, we used mass spectrometry to analyze human myc-tagged α-tubulin (TUBA1B-myc) proteins purified from HEK293T cells.

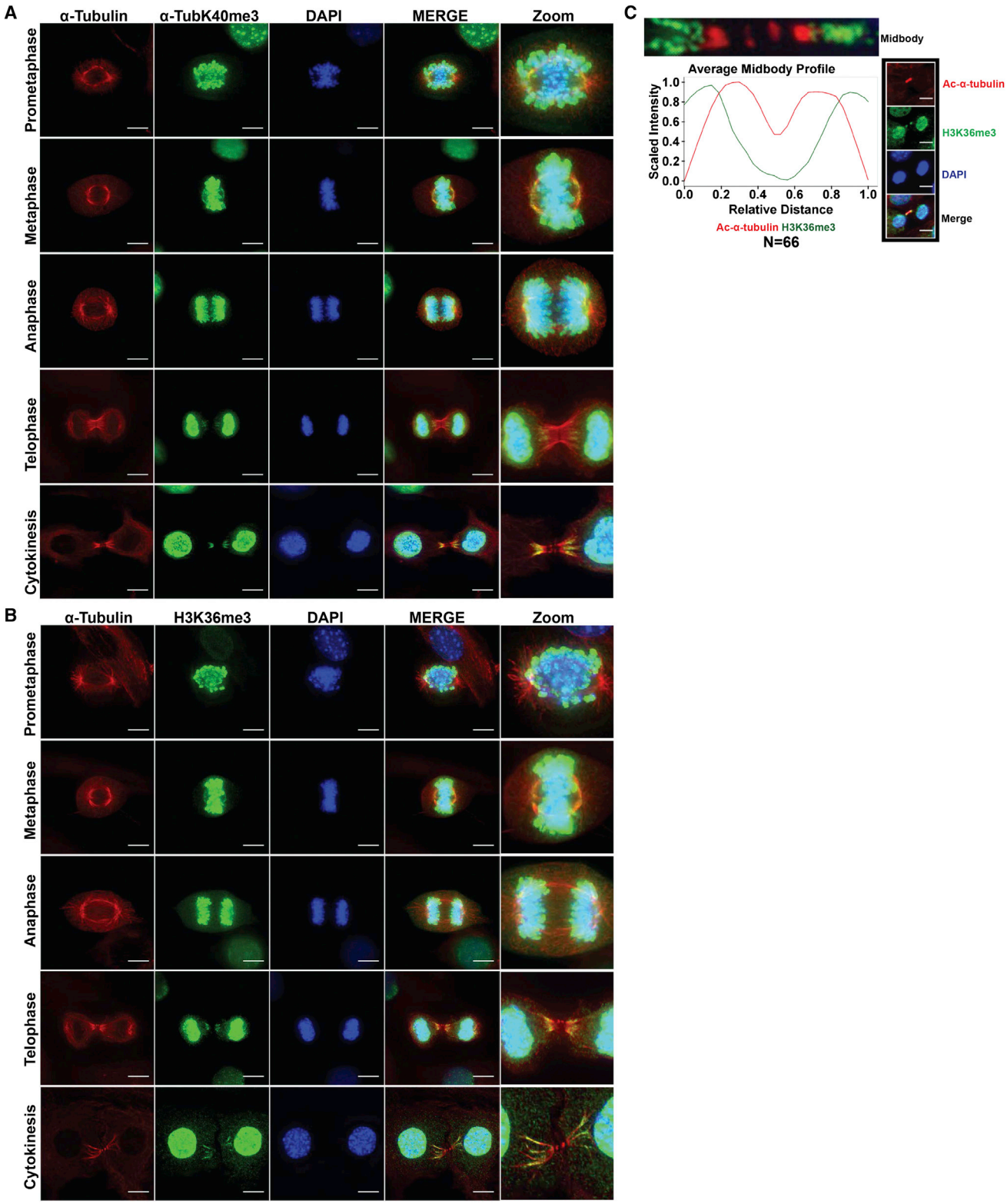

Figure 2. Microtubule Methylation during Mitosis and Cytokinesis in MEFs

(A) Representative images of cells stained using α-tubulin (red) and α-TubK40me3 (green) antibodies, counterstained with DAPI (blue). The far right (Zoom) indicates higher-magnification images for better visualization. Scale bar, 10 μm.

(legend continued on next page)

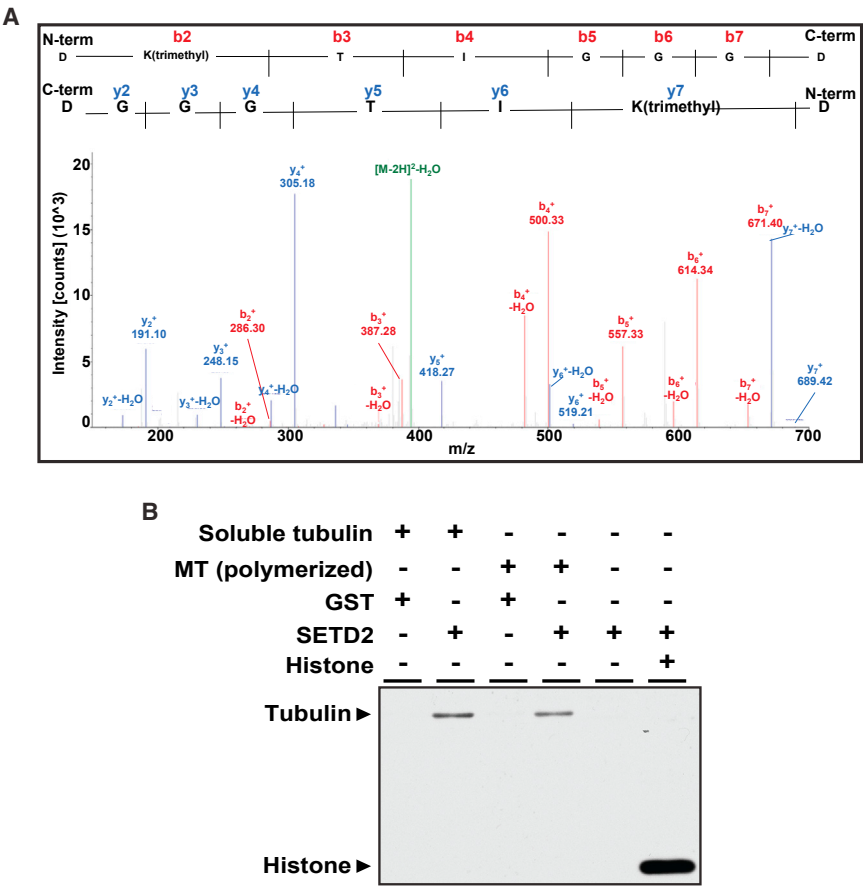

Figure 3. SETD2 Methylates Lysine 40 of α-Tubulin

(A) Mass spectrometry analysis showing trimethylation at K40 on α-tubulin from HEK293T cells. Expected molecular weights of trimethylated peptides from the N terminus and C terminus are shown as peaks in red and blue, respectively.

(B) In vitro methylation of bovine microtubule proteins using recombinant SETD2 and S-[methyl-3H]-adenosyl-L-methionine (SAM) as a methyl donor.

See also Figure S4.

Trimethylation at K40 of α-tubulin was recognized by peaks corresponding to calculated molecular weights from the N and C terminus of the peptide (Figure 3A). We next determined if α-tubulin could be directly methylated by SETD2. SETD2 is able to add a methyl group to di-methylated lysine to generate H3K36me3, but is also capable of de novo mono- and di-methylation to generate a trimethyl mark (Wagner and Carpenter, 2012; Yuan et al., 2009), indicating SETD2 substrate recognition is not confined to di-methylated lysine residues. Using purified α-tubulin, bovine microtubules, or histones (control) as substrates, in vitro methylation assays revealed that recombinant SETD2 was able to methylate both tubulin proteins and histones (Figures 3B and S4A). Polymerization of microtubules was not required for methylation by SETD2, since SETD2 methylated both soluble tubulin and polymerized microtubules, as well as recombinant α-tubulin protein (Figures 3B and S4A). Together, these data demonstrate that trimethylation of α-tubulin is a new PTM of microtubules and identify SETD2 as a dual-function methyltransferase that can directly methylate both histones and α-tubulin.

SETD2 Is a Mitotic Microtubule Methyltransferase

To definitively determine if SETD2 methylates mitotic microtubules, we generated a line of *Setd2*$^{flox/flox}$ mice, isolated *Setd2*$^{flox/flox}$ MEFs, transfected these cells with a tamoxifen-inducible ER-*Cre* expression vector, and isolated stable *Cre*-expressing cells after selection with blasticidin. *Setd2*$^{flox/flox}$; *ER-Cre* MEFs were treated with 4-hydroxytamoxifen or vehicle, and loss of SETD2 activity was observed by the absence of SETD2 protein (Figure S4B), loss of α-TubK40me3-immunoreactivity of α-tubulin (Figure S4B), and loss of nuclear H3K36me3 immunoreactivity (Figure 4A). Immunostaining with H3K36me3 and α-TubK40me3 antibodies confirmed that methylation of microtubules was lost in *Setd2*-knockout MEFs (Figure 4A).

SETD2 Is Required for Genomic Stability

To examine the impact of loss of *Setd2* during mitosis, we clonally selected stable *Setd2*$^{flox/flox}$*;ER-Cre* MEFs and carried out live-cell imaging. In control cells, the average time in mitosis was 1.4 hr (SD = 0.57, n = 63, and illustrated using time-lapse images in Figure 4B). However, after 4-hydroxytamoxifen treatment and excision of *Setd2*, the average time in mitosis was increased to 2.0 hr (SD = 0.68, n = 37, and illustrated using time-lapse images in Figure 4B), with *Setd2*-null cells taking significantly longer to complete mitosis ($p \leq 0.0001$, unpaired Welch t test) and often failing to undergo cytokinesis, resulting in retained cytoplasmic bridges (Figure 4B) and binucleation (Movie S1).

This phenotype suggested that acute loss of *Setd2* function caused mitotic and/or cytokinesis defects. Consistent with induction of the tetraploid checkpoint (Ganem and Pellman,

(B) Representative images of cells stained using α-tubulin (red) and H3K36me3 (green) antibodies, counterstained with DAPI (blue). The far right (Zoom) indicates higher-magnification images for better visualization. Scale bar, 10 μm.

(C) Quantitative analysis of average fluorescent intensities of midbodies immunostained with H3K36me3 (green curve) and acetylated α-tubulin (red curve) antibodies (n = 66 midbodies, from three independent experiments). Representative image showing H3K36me3 (green), acetylated α-tubulin (red) and DAPI (blue). Scale bar, 10 μm.

See also Figure S2 and S3.

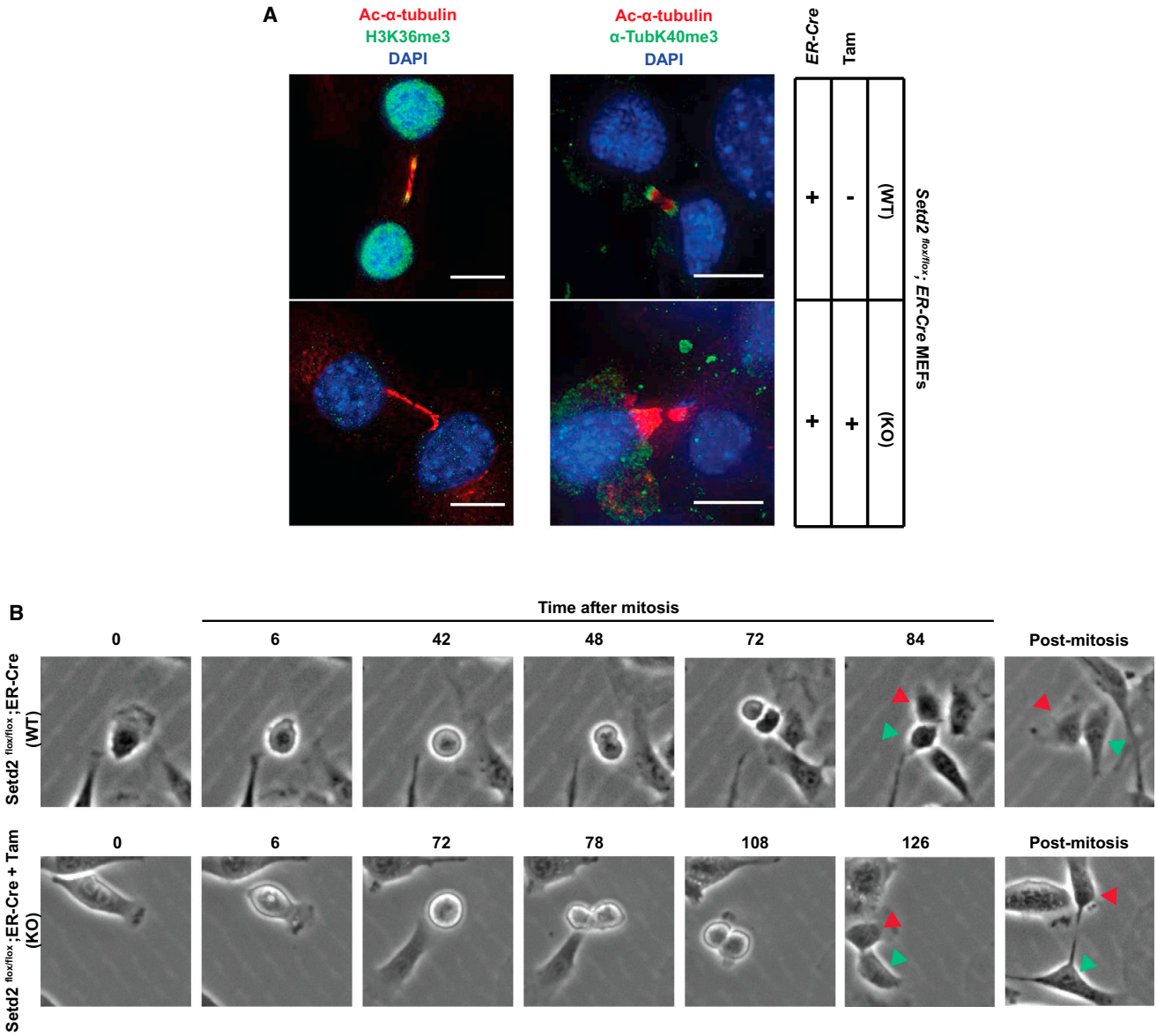

Figure 4. Loss of Methylation on Midbody and Mitosis Delay caused by *Setd2* Ablation

(A) Representative cell images of *Setd2*$^{+/+}$ and *Setd2*$^{-/-}$ cells using H3K36me3 or α-TubK40me3 (green) and acetylated α-tubulin (red) antibodies, counterstained with DAPI (blue). Scale bar, 10 μm. Note that pre-warming the PFA to 37°C significantly reduced cross reactivity of the α-TubK40me3 antibody with chromatin while retaining recognition of the α-TubK40me3 epitope on microtubules, as described in Experimental Procedures.

(B) Live-cell images of *Setd2*$^{+/+}$ and *Setd2*$^{-/-}$ cells undergoing mitosis and cytokinesis. Red and green arrowheads denote corresponding cells tracked during cell division.

See also Figure S4.

2007), tamoxifen-induced excision of *Setd2* caused dramatic increase in the sub-G1 population, and death of *Setd2*-null cells (Figure S5A). When we analyzed the DNA content of clonally derived *Setd2*$^{flox/flox}$ MEFs stably expressing tamoxifen-inducible ER-*Cre* (S4 cells) by flow cytometry after exclusion of the majority of the sub-G1 population (Figures S5B and S5C), we observed increased ploidy, with ~30% of S4 cells becoming polyploid (>4N complement of DNA) upon loss of *Setd2* compared to ~14% of controls (Figure 5A). To eliminate the possibility that the observed increase in >4N DNA was due to cell aggregation, we used automated confocal microscopy to capture images from 3,000 cells 72 hr after *Cre*-mediated excision of *Setd2* and quantitated DAPI fluorescence intensities and DAPI staining area by dot plot using algorithms developed in Pipeline Pilot (Accelrys) (Figure 5B). Consistent with the flow cytometry data, polyploidy in *Setd2*-knockout cells (~41%) was significantly higher than controls (~10% and 17% in pharmacologic and genetic controls). To rule out artifacts associated with clonal

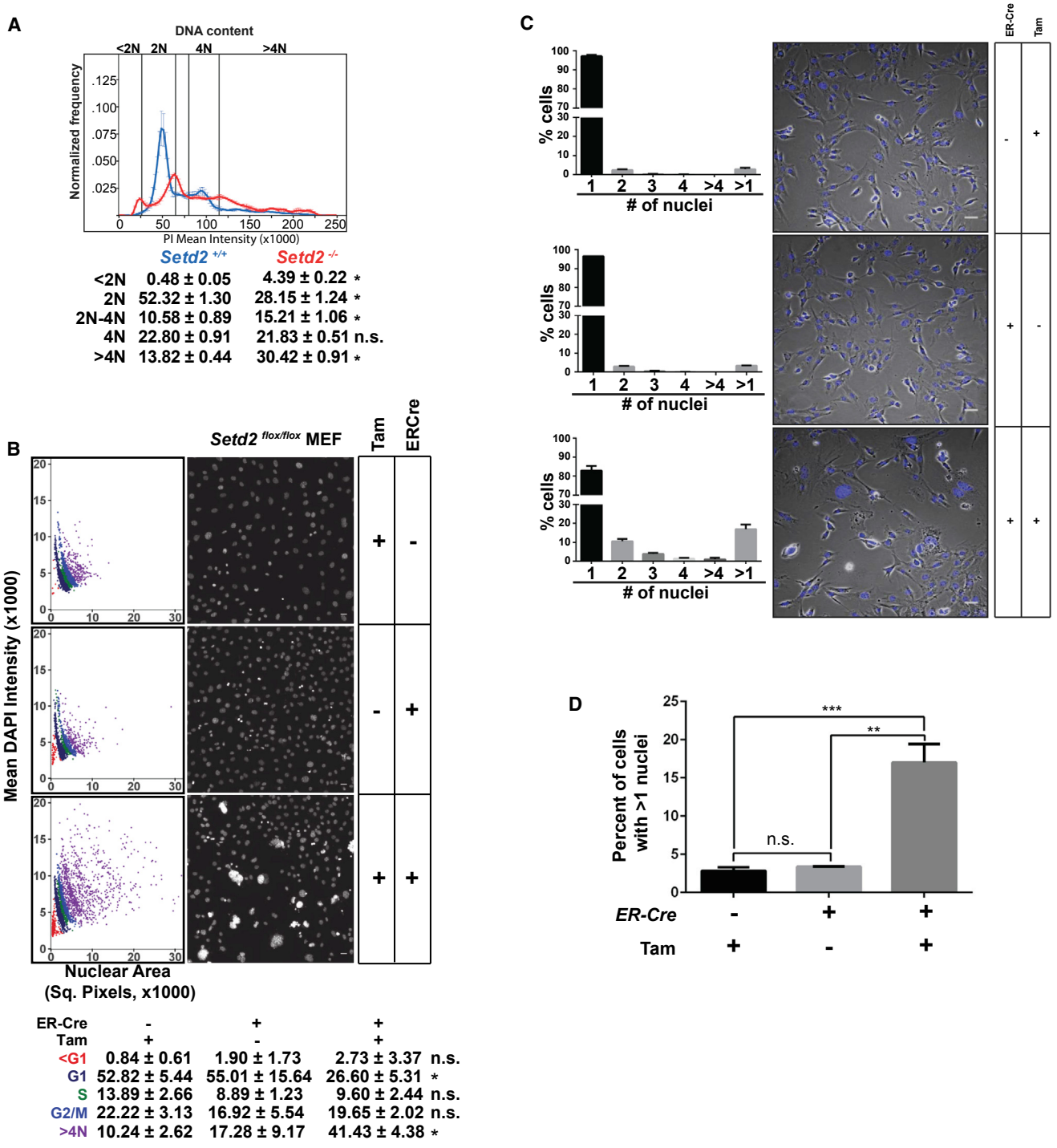

Figure 5. Loss of *Setd2* Induces Polyploidy

(A) FACS analysis of *Setd2*$^{-/-}$ cells (red) and *Setd2*$^{+/+}$ controls (blue). Error bars represent the mean and SD of four biological replicates. *p < 0.0001; n.s., not significant.

(B) Scatterplot of DNA content in *Setd2*-knockout (KO) MEFs with two control cells: *Setd2*$^{flox/flox}$ MEFs treated with 4-hydroxytamoxifen (genetic control) and ER-Cre transfected *Setd2*$^{flox/flox}$ MEFs treated with vehicle (ethanol) (pharmacologic control). Statistics comparing *Setd2* KO to pharmacological control (*p < 0.05). Scale bar, 25 μm, n = 3.

(legend continued on next page)

selection, we also assessed polynucleation in a pool of stably expressing *Setd2*$^{flox/flox}$*;ER-Cre* MEFs after tamoxifen-induced *Cre*-mediated excision of *Setd2*. In three biological replicates counting 500 cells each (1,500 cells), polynucleation in *Setd2* knockout cells was significantly higher than pharmacological and genetic controls (Figures 5C and 5D). Together, these data demonstrated that loss of *Setd2* led to an increase in ploidy and polynucleation.

SETD2 Is Required for Normal Mitosis and Cytokinesis

To examine the mitotic defects caused by loss of SETD2 activity in more detail, we used automated confocal microscopy to examine *Setd2*$^{flox/flox}$*;ER-Cre* MEF clones 72 hr following *Cre*-mediated excision of *Setd2*. Images of mitotic cells were obtained and abnormal mitotic events were identified (Figure 6A) and quantified for n = 191 *Setd2*$^{+/+}$ cells and n = 216 *Setd2*$^{-/-}$ cells (Figure 6B). A significant increase in mitotic and cytokinesis defects was observed following *Setd2* loss, including a failure of chromosomes to congress and an increase in multipolar spindles at prometaphase, lagging chromosomes at anaphase, and chromosomal bridges at cytokinesis. An increase in micronuclei was also observed in *Setd2*$^{-/-}$ cells. This suggested that loss of the α-TubK40me3 mark was responsible for these defects, as other known microtubule PTMs were still present in the spindles of *Setd2*$^{-/-}$ cells (Figure S6).

Loss of SETD2 α-Tubulin Methylation Causes Mitotic and Cytokinesis Defects

As a non-redundant histone methyltransferase, loss of SETD2 results in an absence of H3K36me3, making it at least a formal possibility that mitotic defects observed in *SETD2* null cells occurred secondary to loss of H3K36me3 and disrupted epigenomic programming. To explore this possibility, RNA-sequencing studies were performed on *SETD2*-proficient and *SETD2*-disrupted (via TALEN) 786-0 and HKC (human kidney proximal tubule epithelial) cells (Figure S7). In two biological replicates each for *SETD2*-disrupted 786-0 and HKC cells, as compared with wild-type cells, analysis of differentially expressed genes meeting $p < 0.05$ threshold for significance showed no pathways were consistently observed to be enriched upon loss of SETD2 in these cells (Figure S7).

Next, a series of rescue experiments were performed in 786-0 cells in which *SETD2* had been deleted and then clones selected to re-express an N-terminal truncated (but functional) wild-type (tSETD2-WT), a pathogenic catalytically dead SET-domain mutation (tSETD2-R1625C), or a pathogenic SRI-domain mutation (tSETD2-R2510H). The Set2 Rpb1 interacting (SRI) domain of SETD2 is thought to interact with Pol II during transcription and "marking" of histones by SETD2 (Kizer et al., 2005; Rebehmed et al., 2014). Many pathogenic mutations in this domain have been noted in RCC, suggesting that in addition to the SET domain, this domain plays an important, albeit not completely characterized, role in SETD2 function. As shown in Figure 7A, H3K36me3 histone methylation disappeared in 786-0 *SETD2*-null cells. Expression of tSETD2-WT restored histone methylation, while the tSETD2-R1625C SET-domain mutant (as expected) failed to restore H3K36me3. Mitotic defects followed a similar pattern: the incidence of mitotic defects was higher in *SETD2*-null 786-0 cells relative to the parental cells ($p < 0.0001$), and tSETD2-WT, but not tSETD2-R1625C SET-domain mutant ($p < 0.0001$), rescued this increase in mitotic defects (Figures 7B and 7C). Importantly, while the tSETD2-R2510H SRI-domain mutant fully rescued H3K36me3 to levels equivalent to tSETD2-WT, it was not able to rescue mitotic defects in 786-0 *SETD2*-null cells (Figures 7B and 7C). The tSETD2-R2510H SRI-domain mutant was also unable to rescue K40me3 of α-tubulin (Figure 7D), even when expressed at an equivalent level with tSETD2-WT (Figure 7D), consistent with microtubule methylation defects driving genomic instability in these cells. Together, these data separating loss of histone methylation from genomic instability point to SETD2 methylation of microtubules as being critical for proper mitosis and cytokinesis.

DISCUSSION

Given the differential expression of tubulin isotypes in specific cells and tissues and the identification of several PTMs of tubulin subunits within the microtubule polymer, the concept of a tubulin code has been suggested (Verhey and Gaertig, 2007), parlaying the histone code hypothesis that chromatin structure and gene expression are regulated by a constellation of PTMs (Jenuwein and Allis, 2001; Strahl and Allis, 2000). Although identifying the readers, writers, and erasers of both the tubulin and histone codes is a focus of much research, they have heretofore appeared to be distinct. We report here the identification of methylation as a modification of α-tubulin within microtubules, thus identifying methylation as critical component of the tubulin code. Furthermore, we identified SETD2 as an α-tubulin methyltransferase, defining SETD2 as a dual-function methyltransferase and writer required for the integrity of both the histone and tubulin codes. Although dual function chromatin and cytoskeleton remodelers have not been previously identified, it is possible that other readers, writers, and erasers of the histone code may also have functions associated with the cytoskeleton. Indeed, while we find acute loss of SETD2 leads to loss of microtubule methylation, often accompanied by catastrophic microtubule defects, with prolonged selection, we have been able to isolate SETD2-null cell lines, suggesting the possibility that other methyltransferase(s) may be able to substitute for SETD2 to provide a similar function.

The finding that microtubules are methylated at K40 of α-tubulin, the same site used for acetylation, suggests that methylation and acetylation have opposing functionality for microtubules. There is precedent for acetylation and methylation at a single histone lysine residue to provide mutually exclusive regulatory events. Acetylation of histone H3 at lysine 9

(C) Number of nuclei in *Setd2* KO and with control MEFs. Cells were stained with DAPI and the nuclear content of ~1,500 cells (~500 cells in three independent experiments) was counted manually from multiple confocal images. Scale bar, 50 μm. n = 3.
(D) Percentage of cells (from Figure 5C) with more than one nucleus. **p = 0.0012, ***p = 0.0009. Error bars represent SEM.
See also Figure S5.

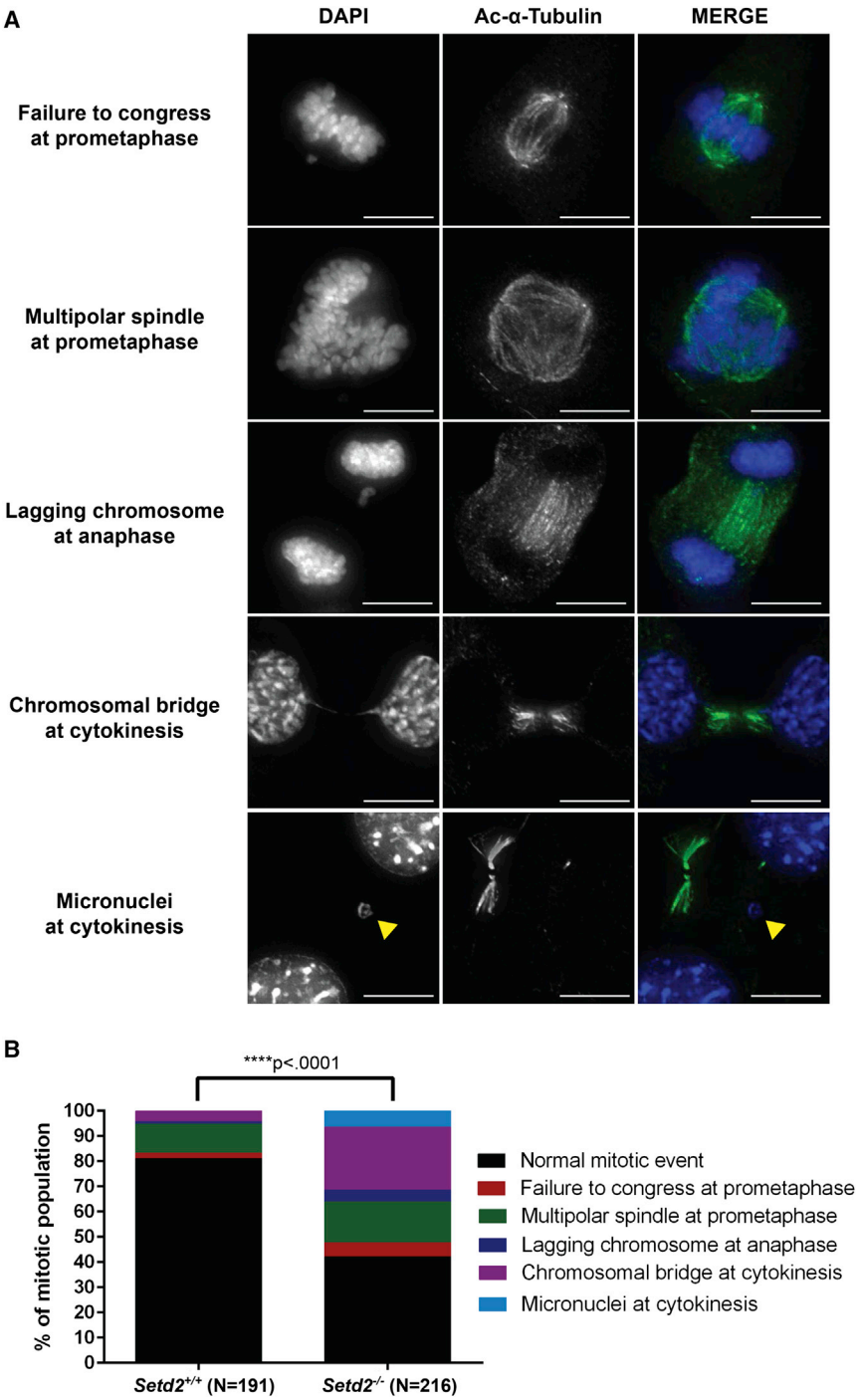

Figure 6. Mitotic and Cytokinesis Defects Induced by Loss of *Setd2*

(A) Representative images of mitotic and cytokinesis defects in *Setd2* KO MEFs using an acetylated α-tubulin (green) antibody and counterstained with DAPI (blue). Scale bar, 10 μm.

(B) Quantitation of abnormal mitotic events in $Setd2^{+/+}$ control and $Setd2^{-/-}$ cells. N, number of dividing cells counted. ****p < 0.0001.

See also Figure S6.

(H3K9ac) activates transcription, while di-and trimethylation of this same lysine repress transcription (Latham and Dent, 2007). Similarly, mutually exclusive acetylation/methylation occurs on H3K14, H3K23, H3K27, H3K36, H4K12, H4K20, and H2BK5 (Latham and Dent, 2007).

α-Tubulin K40 acetylation is associated with certain extraordinarily stable microtubules, including some cytoplasmic microtubules, the axoneme of cilia, and microtubules in neuronal axons. It is thus tempting to speculate that methylation may serve an opposing function, regulating microtubule depolymerization or destruction during mitosis. However, α-TubK40ac is not directly responsible for microtubule stability (Perdiz et al., 2011); some highly acetylated spindle microtubules are also highly dynamic. We thus propose that α-TubK40ac and α-TubK40me3 may recruit different readers to the microtubule shaft and minus ends, respectively, in order to regulate different microtubule-based activities. For example, it was recently shown that detyrosination of spindle microtubules provides an epigenetic mark that is read by the kinesin-7 family motor CENP-E during chromosome congression to the equator (Barisic et al., 2015). As cells proceed toward cytokinesis, α-TubK40me3 likely also recruits reader proteins to the spindle midzone and the midbody. No proteins are known to localize specifically to the minus ends of these microtubules (Green et al., 2012), but the defects seen upon loss of *Setd2* suggest that microtubule methylation maybe critical for activation of the NoCut checkpoint (Agromayor and Martin-Serrano, 2013) and recognition by readers to complete cytokinesis.

What might be the consequences in disease settings such as cancer for cells that lose SETD2? Loss of SETD2 function occurs in ~20% of human renal cell carcinomas (RCCs) (Gerlinger et al., 2012). In some tumors, loss of SETD2 occurs as a subclonal alteration, with tumors exhibiting loss of this methyltransferase having a more aggressive phenotype and worse prognosis (Bi et al., 2016; Cancer Genome Atlas Research Network, 2013; Hakimi et al., 2013; Ho et al., 2016a, 2016b; Kovac et al., 2015; Liao et al., 2015; Liu et al., 2015). A high rate of *SETD2* mutation has also been observed in bladder and lung cancer (Cerami et al., 2012; Gao et al., 2013) and *SETD2* is also mutated in T cell acute lymphoblastic leukemia (Zhang et al., 2012) and acute leukemia (6%) (Zhu et al., 2014).

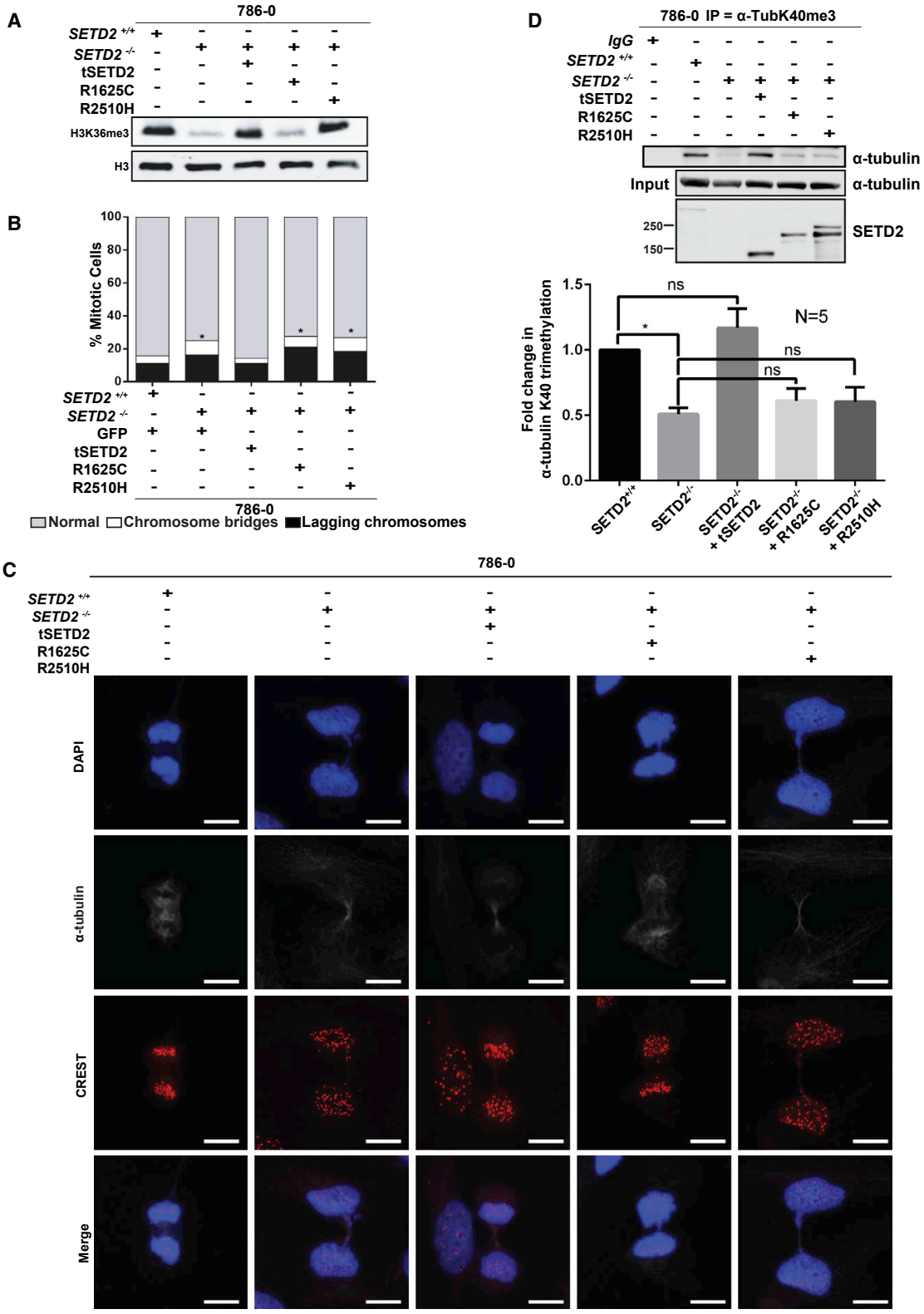

Figure 7. SETD2 SRI Mutant Rescues Histone Methylation, but Not Tubulin Methylation or Mitotic Defects

(A) Western blot analyses using histone extracts from parental 786-0 cells, *SETD2*-null 786-0 cells, or *SETD2*-null 786-0 cells expressing tSETD2 (truncated SETD2 with intact methylation activity), R1625C mutant (SET domain mutant), or R2510H (SRI domain mutant).

(legend continued on next page)

Similarly, SETD2 loss has been associated with more aggressive gastrointestinal (GI) stromal tumors (GIST) (Huang et al., 2015) and high-grade gliomas (Fontebasso et al., 2013; Huether et al., 2014). Recurrent loss-of-function SETD2 mutations are also observed in leukemia (Zhu et al., 2014), which, interestingly, are most commonly truncating mutations leading to loss of the SRI domain. SETD2 mutations are also enriched in relapsed pediatric leukemias (Mar et al., 2014), suggesting therapy supplies a selective pressure for mutation due to loss of this chromatin remodeler and others, leading these authors to suggest that SETD2 inactivation may confer a mutator phenotype that increases mutational diversity, adaptability, and clonal survival, foreshadowing the genomic instability we see with loss of SETD2.

In this regard, H3K36me3 has recently been shown to play important roles in DNA repair (Aymard et al., 2014; Li et al., 2013), and the absence of H3K36me3 is associated with chromatin organizational changes (Simon et al., 2014). These studies suggested a protective role for SETD2 in maintaining genomic stability and identified a requirement for H3K36me3 in double-strand-break resection and homologous recombination repair (Carvalho et al., 2014; Pfister et al., 2014), as well as nucleosome stabilization and suppression of replication stress (Kanu et al., 2015). However, a role for mitotic defects resulting from loss of SETD2 functioning as a driver of genomic instability is a previously unappreciated mechanism by which loss of this methyltransferase may contribute to cancer development and progression. In this regard, clear cell and papillary RCCs have relatively low mutational loads (Alexandrov et al., 2013; Lawrence et al., 2013), suggesting an alternative mechanism may exist by which SETD2 maintains genomic stability. Our data point to an additional and heretofore unknown mechanism by which SETD2 participates in genomic stability via its function as a microtubule methyltransferase and implicate the SRI domain of SETD2 in its function as an α-tubulin methyltransferase. The SRI domain of SETD2 binds the phosphorylated C-terminal domain of Pol II (Kizer et al., 2005; Rebehmed et al., 2014), and pathogenic mutations in the SRI domain of SETD2 have been seen in cancers such as RCC and acute lymphoblastic leukemia (Cancer Genome Atlas Research Network, 2013; Mar et al., 2014). While deletion of the SRI domain abrogates SETD2 histone methyltransferase activity, less is known regarding the impact of SRI missense mutations. Data indicating that a pathogenic SRI mutation causes loss of microtubule, but not histone, methylation is potentially significant, as they suggests that loss of microtubule methylation may participate in tumorigenesis even in cells that retain H3K36me3 of chromatin.

In conclusion, the discovery that SETD2 is a dual-function methyltransferase for histones and microtubules sets the stage for future studies identifying the readers and erasers of K40me3 on microtubules and determining whether other epigenetic readers, writers, and erasers also impinge on the cytoskeleton. These studies now open the door to understanding regulation and cross-talk between the cytoskeleton and epigenome and the role of SETD2 in both normal and pathophysiological conditions such as cancer.

EXPERIMENTAL PROCEDURES

Cell Culture and Generation of *Setd2*-Null *Setd2*$^{flox/flox}$ Mouse Embryonic Fibroblasts

Setd2$^{flox/flox}$ MEFs were generated from 13.5 days postcoitum (d.p.c.) embryos of *Setd2*$^{flox/flox}$ mice. The cells were spontaneously immortalized via serial passaging. The immortalized cells were transfected with an *ER-Cre* vector expressing Cre recombinase fused with a mutated ligand-binding domain for the human estrogen receptor (ER-Cre). Cells expressing this ER-Cre were cultured in phenol-red-free media (DMEM, high glucose, and HEPES, with no phenol red) supplemented with sodium pyruvate and GlutaMAX (Thermo Fisher Scientific) to prevent any spontaneous activation of the Cre recombinase by estrogenic compounds found in phenol-red-containing media. Stable cell lines expressing ER-Cre were generated by selection using 5 μg/ml blasticidin (Thermo Fisher Scientific). Parental *Setd2*$^{flox/flox}$ MEFs treated with 4-hydroxytamoxifen (the active metabolite of tamoxifen; Sigma-Aldrich) and *Setd2*$^{flox/flox}$ MEFs transfected with ER-Cre, treated with vehicle (0.01% ethanol), were used to controls. *Setd2*$^{flox/flox}$ MEFs expressing ER-Cre were treated with 3 μM 4-hydroxytamoxifen for 3–5 days for efficient *Setd2* knockout. All mice were generated and maintained in an Association for Assessment and Accreditation of Laboratory Medical Care (AAALAC) accredited facility and approved by the Texas A&M University Health Science Center institutional animal care and use committee (IACUC).

Generation of Anti-α-TubK40me3 Antibody

The α-TubK40me3 antibody was generated in rabbit using trimethylated K40 peptide (Ac-GQMPSD(KMe3)TIGGGDC-amide) conjugated to KLH as an immunogen (Covance). α-TubK40me3-specific antibody was purified using serial columns coupled with unmethylated and trimethylated K40 peptide.

Immunocytochemistry

Cells were cultured on coverslips and immediately fixed using 4% paraformaldehyde solution in PEM/PEG buffer (80 mM PIPES [pH7.0], 1 mM EGTA, 1 mM $MgCl_2$, and 4% w/v PEG 8000) at room temperature for 30 min (because we failed to observe a robust signal for methylation of microtubules using a shorter, more conventional 15-min fixation), followed by permeabilization using a 0.5% Triton X-100 solution in PEM/PEG buffer for 30 min. We found nonspecific chromatin immunostaining with α-TubK40me3 antibody was reduced by fixation at 37°C using pre-warmed 4% paraformaldehyde solution in PEM/PEG buffer. See Supplemental Experimental Procedures for details.

Statistics

Statistical significance was determined as indicated in Supplemental Experimental Procedures and described in detail in Motulsky (2016).

SUPPLEMENTAL INFORMATION

Supplemental Information includes Supplemental Experimental Procedures, seven figures, and one movie and can be found with this article online at http://dx.doi.org/10.1016/j.cell.2016.07.005.

(B) Mitotic defects including chromosome bridges (white) and lagging chromosomes (black) quantitated for cells from three technical replicates, in each of two biologically independent experiments, for a total of 200 cells for each condition (*$p < 0.0001$).
(C) Representative images of cells stained using α-tubulin (gray), centromere (CREST, red) antibodies, and DAPI (blue). Scale bar, 10 μm.
(D) Immunoprecipitation of cytoplasmic fraction using lysates from (A) with the α-TubK40me3 antibody and immunoblotted using a α-tubulin antibody. In the immunoblot using SETD2 antibody, the tSETD2-2A-GFP fusion protein was autocleaved to tSETD2 and GFP by self-cleaving 2A peptide after translation. The amounts of α-tubulin K40 trimethylation were quantitated by analyzing band intensities in five independent experiments ($n = 5$). *$p < 0.05$; error bars denote SEM. See also Figure S7.

AUTHOR CONTRIBUTIONS

Conceptualization, C.L.W. and I.Y.P.; Methodology, C.L.W., I.Y.P., and R.T.P.; Validation, D.N.T., K.E.H., and Y.-C.C.; Formal Analysis, R.T.P.; Investigation, I.Y.P., R.T.P., D.N.T., I.J.D., C.C.F., K.E.H., T.L.B., L.B., and Y.-C.C.; Resources, T.H.H., W.K.R., K.E.H., and Y.-C.C., Writing – Original Draft, C.L.W. and I.Y.P.; Writing – Review and Editing, R.D., C.L.W., I.Y.P., and R.T.P.; Visualization, R.T.P. and I.Y.P.; Supervision, C.L.W., R.D., K.V., W.K.R., M.T.B., and E.J.; Project Administration, C.L.W., I.Y.P., R.T.P., and R.D.; Funding Acquisition, C.L.W., T.H.H., K.J.V., W.K.R., M.T.B., and E.J.

ACKNOWLEDGMENTS

We thank Dr. Claire Walczak (University of Indiana) for valuable discussions concerning mitotic defects, Tia Berry and Xuefei Tong for technical assistance, Austin Hepperla (UNC Chapel Hill) for designing the pipeline used to align the RNA-sequencing data, and Dr. Sung Yun Jung (Baylor College of Medicine) for mass spectrometry analysis. This work was supported in part by grants from the Robert E. Welch Foundation (BE-0023), the NIH (RC2ES018789, R01ES008263, R01ES023206, R01CA214052, and P30ES023512) and the Cancer Prevention and Research Institute of Texas (CPRIT, DP150086) to C.L.W.; grant R01GM070862 to K.J.V.; grant R01CA198482 and R01CA214052 to W.K.R. and I.J.D.; a V Foundation for Cancer Research award (T2012-008) to W.K.R.; grant R01CA166447 to I.J.D.; grant T32 GM008719 and NRSA award F30 CA192643-02 to C.C.F.; grant CPRIT RP110471 to M.T.B.; grant K12CA90628 and a Gerstner Family Career Development Award to T.H.H.; and NIH/NCI grant P30CA016672 to E.J.

Received: January 7, 2016
Revised: May 13, 2016
Accepted: June 30, 2016
Published: August 11, 2016

REFERENCES

Agromayor, M., and Martin-Serrano, J. (2013). Knowing when to cut and run: mechanisms that control cytokinetic abscission. Trends Cell Biol. *23*, 433–441.

Alexandrov, L.B., Nik-Zainal, S., Wedge, D.C., Aparicio, S.A., Behjati, S., Biankin, A.V., Bignell, G.R., Bolli, N., Borg, A., Børresen-Dale, A.L., et al.; Australian Pancreatic Cancer Genome Initiative; ICGC Breast Cancer Consortium; ICGC MMML-Seq Consortium; ICGC PedBrain (2013). Signatures of mutational processes in human cancer. Nature *500*, 415–421.

Aymard, F., Bugler, B., Schmidt, C.K., Guillou, E., Caron, P., Briois, S., Iacovoni, J.S., Daburon, V., Miller, K.M., Jackson, S.P., and Legube, G. (2014). Transcriptionally active chromatin recruits homologous recombination at DNA double-strand breaks. Nat. Struct. Mol. Biol. *21*, 366–374.

Barisic, M., Silva e Sousa, R., Tripathy, S.K., Magiera, M.M., Zaytsev, A.V., Pereira, A.L., Janke, C., Grishchuk, E.L., and Maiato, H. (2015). Mitosis. Microtubule detyrosination guides chromosomes during mitosis. Science *348*, 799–803.

Bi, M., Zhao, S., Said, J.W., Merino, M.J., Adeniran, A.J., Xie, Z., Nawaf, C.B., Choi, J., Belldegrun, A.S., Pantuck, A.J., et al. (2016). Genomic characterization of sarcomatoid transformation in clear cell renal cell carcinoma. Proc. Natl. Acad. Sci. USA *113*, 2170–2175.

Cancer Genome Atlas Research Network (2013). Comprehensive molecular characterization of clear cell renal cell carcinoma. Nature *499*, 43–49.

Carvalho, S., Vítor, A.C., Sridhara, S.C., Martins, F.B., Raposo, A.C., Desterro, J.M., Ferreira, J., and de Almeida, S.F. (2014). SETD2 is required for DNA double-strand break repair and activation of the p53-mediated checkpoint. eLife *3*, e02482.

Cerami, E., Gao, J., Dogrusoz, U., Gross, B.E., Sumer, S.O., Aksoy, B.A., Jacobsen, A., Byrne, C.J., Heuer, M.L., Larsson, E., et al. (2012). The cBio cancer genomics portal: an open platform for exploring multidimensional cancer genomics data. Cancer Discov. *2*, 401–404.

Chen, Z., Zang, J., Kappler, J., Hong, X., Crawford, F., Wang, Q., Lan, F., Jiang, C., Whetstine, J., Dai, S., et al. (2007). Structural basis of the recognition of a methylated histone tail by JMJD2A. Proc. Natl. Acad. Sci. USA *104*, 10818–10823.

Edmunds, J.W., Mahadevan, L.C., and Clayton, A.L. (2008). Dynamic histone H3 methylation during gene induction: HYPB/Setd2 mediates all H3K36 trimethylation. EMBO J. *27*, 406–420.

Fontebasso, A.M., Schwartzentruber, J., Khuong-Quang, D.A., Liu, X.Y., Sturm, D., Korshunov, A., Jones, D.T., Witt, H., Kool, M., Albrecht, S., et al. (2013). Mutations in SETD2 and genes affecting histone H3K36 methylation target hemispheric high-grade gliomas. Acta Neuropathol. *125*, 659–669.

Ganem, N.J., and Pellman, D. (2007). Limiting the proliferation of polyploid cells. Cell *131*, 437–440.

Gao, J., Aksoy, B.A., Dogrusoz, U., Dresdner, G., Gross, B., Sumer, S.O., Sun, Y., Jacobsen, A., Sinha, R., Larsson, E., et al. (2013). Integrative analysis of complex cancer genomics and clinical profiles using the cBioPortal. Sci. Signal. *6*, pl1.

Gerlinger, M., Rowan, A.J., Horswell, S., Larkin, J., Endesfelder, D., Gronroos, E., Martinez, P., Matthews, N., Stewart, A., Tarpey, P., et al. (2012). Intratumor heterogeneity and branched evolution revealed by multiregion sequencing. N. Engl. J. Med. *366*, 883–892.

Green, R.A., Paluch, E., and Oegema, K. (2012). Cytokinesis in animal cells. Annu. Rev. Cell Dev. Biol. *28*, 29–58.

Guo, A., Gu, H., Zhou, J., Mulhern, D., Wang, Y., Lee, K.A., Yang, V., Aguiar, M., Kornhauser, J., Jia, X., et al. (2014). Immunoaffinity enrichment and mass spectrometry analysis of protein methylation. Mol. Cell. Proteomics *13*, 372–387.

Hakimi, A.A., Ostrovnaya, I., Reva, B., Schultz, N., Chen, Y.B., Gonen, M., Liu, H., Takeda, S., Voss, M.H., Tickoo, S.K., et al. (2013). Adverse outcomes in clear cell renal cell carcinoma with mutations of 3p21 epigenetic regulators BAP1 and SETD2: a report by MSKCC and the KIRC TCGA research network. Clin. Cancer Res. *19*, 3259–3267.

Ho, T.H., Kapur, P., Joseph, R.W., Serie, D.J., Eckel-Passow, J.E., Tong, P., Wang, J., Castle, E.P., Stanton, M.L., Cheville, J.C., et al. (2016a). Loss of histone H3 lysine 36 trimethylation is associated with an increased risk of renal cell carcinoma-specific death. Mod. Pathol. *29*, 34–42.

Ho, T.H., Park, I.Y., Zhao, H., Tong, P., Champion, M.D., Yan, H., Monzon, F.A., Hoang, A., Tamboli, P., Parker, A.S., et al. (2016b). High-resolution profiling of histone h3 lysine 36 trimethylation in metastatic renal cell carcinoma. Oncogene *35*, 1565–1574.

Hu, M., Sun, X.J., Zhang, Y.L., Kuang, Y., Hu, C.Q., Wu, W.L., Shen, S.H., Du, T.T., Li, H., He, F., et al. (2010). Histone H3 lysine 36 methyltransferase Hypb/Setd2 is required for embryonic vascular remodeling. Proc. Natl. Acad. Sci. USA *107*, 2956–2961.

Huang, K.K., McPherson, J.R., Tay, S.T., Das, K., Tan, I.B., Ng, C.C., Chia, N.Y., Zhang, S.L., Myint, S.S., Hu, L., et al. (2015). SETD2 histone modifier loss in aggressive GI stromal tumours. Gut. Published online September 3, 2015. http://dx.doi.org/10.1136/gutjnl-2015-309482.

Huether, R., Dong, L., Chen, X., Wu, G., Parker, M., Wei, L., Ma, J., Edmonson, M.N., Hedlund, E.K., Rusch, M.C., et al. (2014). The landscape of somatic mutations in epigenetic regulators across 1,000 paediatric cancer genomes. Nat. Commun. *5*, 3630.

Janke, C. (2014). The tubulin code: molecular components, readout mechanisms, and functions. J. Cell Biol. *206*, 461–472.

Jenuwein, T., and Allis, C.D. (2001). Translating the histone code. Science *293*, 1074–1080.

Kanu, N., Grönroos, E., Martinez, P., Burrell, R.A., Yi Goh, X., Bartkova, J., Maya-Mendoza, A., Mistrík, M., Rowan, A.J., Patel, H., et al. (2015). SETD2 loss-of-function promotes renal cancer branched evolution through replication stress and impaired DNA repair. Oncogene *34*, 5699–5708.

Kizer, K.O., Phatnani, H.P., Shibata, Y., Hall, H., Greenleaf, A.L., and Strahl, B.D. (2005). A novel domain in Set2 mediates RNA polymerase II interaction

and couples histone H3 K36 methylation with transcript elongation. Mol. Cell. Biol. *25*, 3305–3316.

Kovac, M., Navas, C., Horswell, S., Salm, M., Bardella, C., Rowan, A., Stares, M., Castro-Giner, F., Fisher, R., de Bruin, E.C., et al. (2015). Recurrent chromosomal gains and heterogeneous driver mutations characterise papillary renal cancer evolution. Nat. Commun. *6*, 6336.

Kwok, B.H., and Kapoor, T.M. (2007). Microtubule flux: drivers wanted. Curr. Opin. Cell Biol. *19*, 36–42.

Latham, J.A., and Dent, S.Y. (2007). Cross-regulation of histone modifications. Nat. Struct. Mol. Biol. *14*, 1017–1024.

Lawrence, M.S., Stojanov, P., Polak, P., Kryukov, G.V., Cibulskis, K., Sivachenko, A., Carter, S.L., Stewart, C., Mermel, C.H., Roberts, S.A., et al. (2013). Mutational heterogeneity in cancer and the search for new cancer-associated genes. Nature *499*, 214–218.

Lee, J.S., Smith, E., and Shilatifard, A. (2010). The language of histone crosstalk. Cell *142*, 682–685.

Li, F., Mao, G., Tong, D., Huang, J., Gu, L., Yang, W., and Li, G.M. (2013). The histone mark H3K36me3 regulates human DNA mismatch repair through its interaction with MutSα. Cell *153*, 590–600.

Liao, L., Testa, J.R., and Yang, H. (2015). The roles of chromatin-remodelers and epigenetic modifiers in kidney cancer. Cancer Genet. *208*, 206–214.

Liu, W., Fu, Q., An, H., Chang, Y., Zhang, W., Zhu, Y., Xu, L., and Xu, J. (2015). Decreased expression of SETD2 predicts unfavorable prognosis in patients with nonmetastatic clear-cell renal cell carcinoma. Medicine (Baltimore) *94*, e2004.

Magiera, M.M., and Janke, C. (2013). Investigating tubulin posttranslational modifications with specific antibodies. Methods Cell Biol. *115*, 247–267.

Mar, B.G., Bullinger, L.B., McLean, K.M., Grauman, P.V., Harris, M.H., Stevenson, K., Neuberg, D.S., Sinha, A.U., Sallan, S.E., Silverman, L.B., et al. (2014). Mutations in epigenetic regulators including SETD2 are gained during relapse in paediatric acute lymphoblastic leukaemia. Nat. Commun. *5*, 3469.

Matsuyama, A., Shimazu, T., Sumida, Y., Saito, A., Yoshimatsu, Y., Seigneurin-Berny, D., Osada, H., Komatsu, Y., Nishino, N., Khochbin, S., et al. (2002). In vivo destabilization of dynamic microtubules by HDAC6-mediated deacetylation. EMBO J. *21*, 6820–6831.

Motulsky, H.J. (2016) GraphPad Statistics Guide. Accessed 30 May 2016. http://www.graphpad.com/guides/prism/7/statistics/index.htm (GraphPad Software, Inc.).

Nelson, C.J., Santos-Rosa, H., and Kouzarides, T. (2006). Proline isomerization of histone H3 regulates lysine methylation and gene expression. Cell *126*, 905–916.

Perdiz, D., Mackeh, R., Poüs, C., and Baillet, A. (2011). The ins and outs of tubulin acetylation: more than just a post-translational modification? Cell. Signal. *23*, 763–771.

Pfister, S.X., Ahrabi, S., Zalmas, L.P., Sarkar, S., Aymard, F., Bachrati, C.Z., Helleday, T., Legube, G., La Thangue, N.B., Porter, A.C., and Humphrey, T.C. (2014). SETD2-dependent histone H3K36 trimethylation is required for homologous recombination repair and genome stability. Cell Rep. *7*, 2006–2018.

Rebehmed, J., Revy, P., Faure, G., de Villartay, J.P., and Callebaut, I. (2014). Expanding the SRI domain family: a common scaffold for binding the phosphorylated C-terminal domain of RNA polymerase II. FEBS Lett. *588*, 4431–4437.

Simon, J.M., Hacker, K.E., Singh, D., Brannon, A.R., Parker, J.S., Weiser, M., Ho, T.H., Kuan, P.F., Jonasch, E., Furey, T.S., et al. (2014). Variation in chromatin accessibility in human kidney cancer links H3K36 methyltransferase loss with widespread RNA processing defects. Genome Res. *24*, 241–250.

Song, Y., and Brady, S.T. (2015). Post-translational modifications of tubulin: pathways to functional diversity of microtubules. Trends Cell Biol. *25*, 125–136.

Strahl, B.D., and Allis, C.D. (2000). The language of covalent histone modifications. Nature *403*, 41–45.

Verhey, K.J., and Gaertig, J. (2007). The tubulin code. Cell Cycle *6*, 2152–2160.

Wagner, E.J., and Carpenter, P.B. (2012). Understanding the language of Lys36 methylation at histone H3. Nat. Rev. Mol. Cell Biol. *13*, 115–126.

Walczak, C.E., and Heald, R. (2008). Mechanisms of mitotic spindle assembly and function. Int. Rev. Cytol. *265*, 111–158.

Yuan, W., Xie, J., Long, C., Erdjument-Bromage, H., Ding, X., Zheng, Y., Tempst, P., Chen, S., Zhu, B., and Reinberg, D. (2009). Heterogeneous nuclear ribonucleoprotein L is a subunit of human KMT3a/Set2 complex required for H3 Lys-36 trimethylation activity in vivo. J. Biol. Chem. *284*, 15701–15707.

Zhang, J., Ding, L., Holmfeldt, L., Wu, G., Heatley, S.L., Payne-Turner, D., Easton, J., Chen, X., Wang, J., Rusch, M., et al. (2012). The genetic basis of early T-cell precursor acute lymphoblastic leukaemia. Nature *481*, 157–163.

Zhu, X., He, F., Zeng, H., Ling, S., Chen, A., Wang, Y., Yan, X., Wei, W., Pang, Y., Cheng, H., et al. (2014). Identification of functional cooperative mutations of SETD2 in human acute leukemia. Nat. Genet. *46*, 287–293.